JOURNAL OF VIROLOGY, June 2006, p. 5841–5853 Vol. 80, No. 12
0022-538X/06/$08.00+0 doi:10.1128/JVI.02698-05

Peptide Aptamers That Bind to a Geminivirus Replication Protein Interfere with Viral Replication in Plant Cells†

Luisa Lopez-Ochoa, Jorge Ramirez-Prado,‡ and Linda Hanley-Bowdoin*

Department of Molecular and Structural Biochemistry, North Carolina State University, Raleigh, North Carolina 27695-7622

Received 22 December 2005/Accepted 18 March 2006

The AL1 protein of tomato golden mosaic virus (TGMV), a member of the geminivirus family, is essential for viral replication in plants. Its N terminus contains three conserved motifs that mediate origin recognition and DNA cleavage during the initiation of rolling-circle replication. We used the N-terminal domain of TGMV AL1 as bait in a yeast two-hybrid screen of a random peptide aptamer library constrained in the active site of the thioredoxin A (TrxA) gene. The screen selected 88 TrxA peptides that also bind to the full-length TGMV AL1 protein. Plant expression cassettes corresponding to the TrxA peptides and a TGMV A replicon encoding AL1 were cotransfected into tobacco protoplasts, and viral DNA replication was monitored by semiquantitative PCR. In these assays, 31 TrxA peptides negatively impacted TGMV DNA accumulation, reducing viral DNA levels to 13 to 64% of those of the wild type. All of the interfering aptamers also bound to the AL1 protein of cabbage leaf curl virus. A comparison of the 20-mer peptides revealed that their sequences are not random. The alignments detected seven potential binding motifs, five of which are more highly represented among the interfering peptides. One motif was present in 18 peptides, suggesting that these peptides interact with a hot spot in the AL1 N terminus. The peptide aptamers characterized in these studies represent new tools for studying AL1 function and can serve as the basis for the development of crops with broad-based resistance to single-stranded DNA viruses.

Geminiviruses are a large family of single-stranded DNA viruses with twin icosahedral capsids that infect both monocotyledonous and dicotyledonous plant species. They are divided into four genera, begomoviruses, curtoviruses, topocuviruses, and mastreviruses, based on their genome organization and insect vector specificity (24). Geminivirus-produced diseases cause major economic losses in a broad range of vegetable and field crops, with multiple viruses often contributing to disease in a given crop (47, 50, 53). Geminviruses frequently occur as mixed infections and are often synergistic, leading to increased viral DNA accumulation and increased symptom severity (34). They can also form pseudorecombinants and undergo recombination to form new, more virulent viruses (69). An emerging class of satellite DNA molecules, which encode pathogenicity determinants, also recombine and further contribute to the genetic variability and rapid virus evolution in the field (50, 79).

Geminiviruses replicate through double-stranded DNA (dsDNA) intermediates (31) via a combination of rolling-circle replication and recombination-dependent replication mechanisms (29, 64). They do not encode a DNA polymerase and instead rely on host replication machinery (30–32). Tomato golden mosaic virus (TGMV) is a begomovirus with a bipartite genome. Two of the seven proteins encoded by TGMV are involved in viral replication. AL1 (also called AC1, C1, and Rep) is essential for replication (21), while AL3 (also called AC3, C3, and REn) enhances viral DNA accumulation (80). AL1 is a multifunctional protein that mediates virus-specific recognition of its cognate origin (25), initiates and terminates plus-strand DNA synthesis within a conserved hairpin motif (46), induces the accumulation of host replication factors in infected cells (30, 55), and is thought to unwind viral DNA in an ATP-dependent manner (63). A variety of protein interactions have been demonstrated for AL1 from TGMV and other geminivirus replication proteins, including the formation of homomultimers (61), interaction with AL3 (75, 76) and coat protein (CP) (49), and binding to several host factors (2, 13, 14, 41). The best-characterized host interaction is the interaction with the retinoblastoma-related protein (pRBR), a key regulator of the cell division cycle and differentiation in plants (4, 42, 51).

The N terminus of AL1 contains the overlapping domains for DNA binding and cleavage/ligation (60, 62). It resembles other DNA binding proteins structurally (12) and includes three conserved motifs, designated motifs I, II, and III, that are characteristic of rolling-circle initiators (39, 43). Motif I (FLTY) is a determinant of dsDNA binding specificity (5, 15). Motif II (HLH) is a metal binding site that may impact protein conformation and/or catalysis. Motif III (YxxKD/E) is the catalytic site for DNA cleavage, with the hydroxyl group of the Y residue forming a covalent bond with the 5′ phosphoryl group of the cleaved DNA strand (46). The aromatic ring of the Y residue is also required for dsDNA binding (60).

A variety of strategies have been applied towards geminivirus resistance, including conventional breeding and transgenic approaches. Conventional breeding has been limited by the available sources of natural resistance, the multigenic nature of the resistance traits, and the time required for a breeding program (54). Several transgenic strategies based on viral se-

* Corresponding author. Mailing address: Department of Molecular and Structural Biochemistry, North Carolina State University, Raleigh, NC 27695-7622. Phone: (919) 515-6663. Fax: (919) 515-2047. E-mail: linda_hanley-bowdoin@ncsu.edu.

† Supplemental material for this article may be found at http://jvi.asm.org/.

‡ Current address: Department of Plant Pathology, North Carolina State University, Raleigh, NC 27695.

quences, including mutant viral proteins, antisense RNAs, and RNA interference constructs, have been evaluated (6, 16, 38, 45, 84). Most of these approaches do not confer high levels of resistance or are limited to cognate and closely related viruses (9, 48). Recently, expression of a recombinant zinc finger protein that binds to the origin of beet curly top virus was shown to confer resistance in plants (74), but this protein is likely to be effective only against viruses with shared origin recognition sequences. Given the complexity and dynamic nature of geminivirus disease complexes, it is essential to develop alternative strategies toward stable and broad-based resistance.

Peptide aptamers are recombinant proteins that bind to and inactivate a protein of interest (18, 36, 37). They have been expressed in eukaryotic cells and at the whole-organism level and have been shown to target protein function (19). Peptide aptamers resemble single-chain antibodies in that they contain constrained peptide sequences that specifically interact with target proteins (26, 36). However, unlike single-chain antibodies (scFv), which are usually isolated in vitro via phage display, peptide aptamers are identified in vivo using stringent yeast dihybrid conditions. As a consequence, the expression problems often associated with single-chain antibodies are not generally encountered with peptide aptamers.

Peptide aptamers are especially well suited for the targeting of noncellular factors like viral proteins. An aptamer that binds to the hepatitis B virus core protein and inhibits viral capsid formation and replication has strong antiviral activity in cultured liver cells (10). Peptides that target the nucleoprotein P complex of rabies virus inhibit viral replication in vitro and infection in cell culture (67). Peptide aptamers that bind to the E6 and E7 proteins of human papillomavirus and block their antiapoptotic activities result in the specific elimination of human papillomavirus-positive cancer cells (11, 57). In plants, a single-chain antibody directed against a conserved domain in the viral RNA-dependent RNA polymerase inhibits tomato bushy stunt virus replication in vitro and infection in transgenic plants (8). Single-chain antibodies against cucumber mosaic virus particles also confer resistance to transgenic plants (82). Expression of β-glucuronidase fusions with virus-derived peptides that target the oligomerization domain of the N protein of the tomato spotted wilt virus in transgenic plants confers resistance to the homologous virus and three other tospoviruses (70). Those studies demonstrated the potential of using antibodies or "antibody-like" molecules to confer broad-based resistance to RNA virus infection in plants. In this paper, we identify constrained peptide aptamers that bind to the AL1 proteins of TGMV and cabbage leaf curl virus (CaLCuV) and interfere with viral replication, a first step towards obtaining broad-based resistance to geminiviruses.

MATERIALS AND METHODS

Yeast plasmids. All the bait and prey plasmids used in this study are listed in Table 1. pNSB1118, the bait plasmid for full-length TGMV AL1 ($TAL1_{1-352}$), was generated by cloning a 1.2-kb fragment with NdeI (trimmed) and BamHI ends from pNSB736 (61) into pEG202 (28) with BamHI and EcoRI (repaired) ends. The same fragment was also ligated into pHybLex/Zeo (Invitrogen) digested with PvuII and BamHI to create pNSB1089. The $TAL1_{1-352}$ coding sequence from pNSB1089 was introduced into pYESTrp2 (Invitrogen) as a SacI/XhoI fragment to create the prey plasmid pNSB970. The bait plasmid for truncated $TAL1_{1-130}$ (pNSB1162) was generated in two steps. First, an 895-bp EcoRI/BamHI fragment from pNSB603 (61) was ligated into the same sites of pNSB1118 to create pNSB1153. pNSB1153 was then digested with NotI, repaired with *Escherichia coli* DNA polymerase (Klenow fragment), and religated to delete an 861-bp sequence encoding the TAL1 C terminus. The bait plasmid (pNSB1122) for full-length CaLCuV AL1 ($CaAL1_{1-349}$) was built by cloning a 1.2-kb BamHI/XhoI fragment from pNSB909 (41) into the same sites of pEG202.

TABLE 1. Yeast dihybrid plasmids

Insert	Cloning vector	Yeast selection[a]	Plasmid
Bait (DBD)			
$TAL1_{1-352}$	pEG202	(−) Histidine	pNSB1118
$TAL1_{1-130}$	pEG202	(−) Histidine	pNSB1162
$CaAL1_{1-349}$	pEG202	(−) Histidine	pNSB1122
GUS	pEG202	(−) Histidine	pNSB1120
Prey (AD)			
$TAL1_{1-352}$	pYESTrp2	(−) Tryptophan	pNSB970
Jun	pYESTrp2	(−) Tryptophan	pYESTrp-Jun
TrxA-GST	pYESTrp2	(−) Tryptophan	pNSB1172

[a] (−) Histidine, medium lacking histidine; (−) Tryptophan, medium lacking tryptophan.

The β-glucuronidase (GUS) coding sequence from pMON10018 (Monsanto) was cloned into pEG202 as a 2.2-kb BglII/NotI fragment to generate the control bait plasmid pNSB1120. An EcoRI/NotI fragment encoding TrxA-glutathione *S*-transferase (GST) from pNSB1166 (described below) was cloned into the same sites of pYESTrp2 to generate pNSB1172, a negative-control prey plasmid.

Plant expression plasmids. TrxA peptide prey plasmids isolated in the $TAL1_{1-352}$ screen were digested with EcoRI/XbaI, and the resulting 412-bp fragments were gel purified and cloned into pMON921 (25). To eliminate the gel purification step during the cloning of aptamers derived from the $AL1_{1-130}$ screen, a polylinker was inserted into pMON921, and the β-lactamase gene was replaced by the aminoglycoside 3′ phosphotransferase (*aphA*) coding sequence, which confers kanamycin resistance. The polylinker was generated by ligating the annealed oligonucleotides LLp27 and LLp28 (Table 2) into pMON921 digested with BglII/BamHI to create pNSB1208. A fragment carrying the *aphA* gene was amplified from pFGC5941 (40) using primers LLp29 and LLp30 (Table 2), digested with SmaI/AatII, and cloned into pNSB1208 cut with DraI/AatII to generate pNSB1226. The N-terminal TrxA (N-TrxA) peptides were cloned into pNSB1226 as EcoRI/BamHI fragments. N-TrxA aptamers with internal EcoRI or BamHI sites (N-3, N-71, N-99, N-123, N-149, and N-153) were cloned into pNSB1226 as PCR-generated EcoRI/SacI or SacI inserts using primers LLp41 and LLp42 (Table 2).

The TrxA-GST control was generated in two steps. First, the RsrII site in the active site of the thioredoxin coding sequence (TrxA) was reconstituted. Two fragments were generated using pJM-1 library DNA as a template in PCRs with primer pairs LLp9/LLp16 and LLp15/LLp12 (Table 2.) The PCR products were digested with RsrII and ligated in vitro. The resulting 414-bp fragment was digested with EcoRI/BamHI and cloned into the same sites of pBSKSII(−) to generate pNSB1151. Both constructs were sequenced to verify the integrity of the TrxA sequence. Oligonucleotides LLp55 and LLp56 (Table 2), carrying a 60-bp sequence of the GST gene, were annealed and ligated into the RsrII site of pNSB1151, creating pNSB1166. An EcoRI/BamHI fragment from pNSB1166 was cloned into the same sites of pMON921 to generate pNSB1168. The expression cassette (pNSB866) corresponding to FQ118, a TAL1 *trans*-dominant-negative mutant, has been described previously (61).

Peptide aptamer screens. The pJM-1 library (18) was amplified by transforming 5 μg plasmid DNA into 1×10^{10} electrocompetent *E. coli* DH10B cells (Invitrogen) and stored at −80°C in 40-ml aliquots containing 5×10^8 CFU/ml (26). Plasmid DNA was extracted using a QIAfilter Plasmid Maxi kit according to the manufacturer's protocols (QIAGEN). *Saccharomyces cerevisiae* strains EGY48 (*MAT his3 trp1 ura3-52 leu2*::*LexA6op-LEU2*) and EGY191 (*MAT his3 trp1 ura3-52 leu2*::*LexA2op-LEU2*) were used for the library screens (22). Plasmid DNA (50 μg) from the library was transformed into the bait strains containing the *lacZ* reporter plasmid pSH18-34 (Invitrogen) (22, 28) and the corresponding bait plasmids. Transformants were plated onto synthetic dropout medium lacking histidine, tryptophan, uracil, and leucine and supplemented with galactose-raffinose (Gal−HWUL) after heat shock and a 4-h incubation at 30°C in liquid medium containing galactose-raffinose and lacking histidine and uracil (26). Recovered yeast colonies were also grown in medium lacking histidine, trypto-

TABLE 2. Oligonucleotides

Oligonucleotide	Target	Sequence[a]	Application
LLp1	5′-AL1 TGMV A	GATGTTTGGCAACCTCCTCTAG	Replication
LLp2	3′-CP TGMV A	GGTCGTTCTTTACCGTTGCAGTAC	Replication
LLp9	5′-pJM-1	TCAATGAGCTCGGTCCTACCCTTATGATGTG	Cloning
LLp10	5′-pJM-1	TTCACCTGACTGACGACAGT	Sequencing
LLp12	3′-pJM-1	ATGGATCCAGGCCTCTGGCGAAGAAGTCC	Cloning
LLp13	5′-pMON921	TCATTTCATTTGGAGAGGACACGC	Sequencing
LLp14	3′-pMON921	CCAATGCCATAATACTCGAACTCA	Sequencing
LLp15	TrxA-2	TACAGCGGTCCGTGCAAAATGATCGCC	Cloning
LLp16	TrxA-1	CGGACCGCACCACTCTGCCCAG	Cloning
LLp27	pMON921	GATCTGAATTCGCGATCTAGAGAGCTCG	Cloning
LLp28	pMON921	GATCCGAGCTCTCTAGATCGCGAATTCA	Cloning
LLp29	5′-aphA	AATTCGGACGTCGCTCCGTCGATACTATGTTATACGCC	Cloning
LLp30	3′-aphA	ATGACCCGGGGACGCTCAGTGGAACGAAAACTCACG	Cloning
LLp39	5′-Npt II	GGCGATAGAAGGCGATGCGCTGCG	Replication
LLp40	3′-Npt II	TGCACGCAGGTTCTCCGGCCGCT	Replication
LLp41	5′-pJM-1	AAGAGCTCAGTACTCCTACCCTTATGATGTGCCA	Cloning
LLp42	3′-pJM-1	TTGAGCTCCTCTGGCGAAGAAGTCCA	Cloning
LLp55	5′-GST 20mer	GTCCGGAGCTCCCTATACTAGGTTATTGGAAAATTAAGGG CCTTGTGCAACCCACTCGCG	Cloning
LLp56	3′-GST 20mer	GACCGCGAGTGGGTTGCACAAGGCCCTTAATTTTCCAATAAC CTAGTATAGGGAGCTCCG	Cloning

[a] Nucleotides used to generate restriction sites for cloning are underlined.

phan, and uracil supplemented with glucose (Glu−HWU) to repress library expression. Activation of the leucine and β-galactosidase reporters was confirmed in growth assays (Gal−HWUL) and filter lift assays (Gal−HWU), respectively (26). pJM-1 plasmids containing the selected aptamers were recovered using the lyticase protocol and QIAGEN Miniprep columns. The plasmids were transformed into *E. coli* strain KC8 (Clontech Yeast Protocols Manual PT3024-1) and selected on minimal M9 medium lacking tryptophan. Recovered plasmids were transferred into *E. coli* DH5α for isolation and retransformed into the yeast baits strains to confirm specific activation with the $TAL1_{1\text{-}352}$ and $TAL1_{1\text{-}130}$ baits and not with the GUS bait. For these assays, 4-μl droplets of 1×10^{-2} dilutions (optical density at 600 nm adjusted to 0.08 to 0.12) of fresh yeast colonies were plated onto Gal−HWUL medium and incubated at 30°C for 3 to 6 days. For sequencing, DNA minipreps were performed using the R.E.A.L. Prep 96 plasmid kit and a Biorobot 9600 apparatus (QIAGEN). Sequencing was performed according to the BigDye Terminator v3.1 method (Applied Biosystems) using a Perkin-Elmer Prism 3700 96-capillary automated DNA sequencer.

Replication interference assays. Protoplasts were isolated from *Nicotiana tabacum* (BY-2) suspension cells, electroporated, and cultured according to previously published methods (25). For the replication interference assays (61), replicon DNA (2 μg) containing a partial tandem copy of TGMV A (pMON1565) (59) was cotransfected with a plant expression cassette (40 μg). Viral DNA accumulation was monitored by either hybridization or semiquantitative PCR. For the hybridization assays, total DNA was extracted 48 h posttransfection, digested with DpnI and XhoI, resolved on 1% agarose gels, and probed with a ^{32}P-labeled DNA corresponding to TGMV A. Double-stranded viral DNA accumulation was quantified by phosphorimage analysis in a minimum of three independent experiments.

For semiquantitative PCR assays, BY-2 cells were harvested 36 h posttransfection and lysed by vortexing using 50 μl of glass beads in 400 μl lysis buffer (50 mM Tris-HCl, pH 7.6, 100 mM NaCl, 50 mM EDTA, 0.5% sodium dodecyl sulfate). The lysates were cleared by centrifugation at 14,000 × *g* for 5 min and extracted using a QIAprep Spin Miniprep kit according to the manufacturer's protocols (QIAGEN). Total DNA was quantified by measuring the A_{260}, and identical amounts were digested overnight with DpnI and subjected to PCR analysis using primers LLp1 and LLp2 (Table 2) for the TGMV A replicon. The amount (12.5 to 200 ng) of total DNA in the reactions was titrated for each experiment. pMON721 plasmid DNA (1 pg), which does not contain TGMV sequences (44), was added to each PCR as an internal control and amplified with primers LLp39 and LLp40 (Table 2). Bands were quantified using ImageJ software (1, 66). PCR efficiency was standardized between reactions as a ratio of the band intensities corresponding to TGMV A DNA and the pMON721 control. Relative replication was determined as the ratio of the normalized intensity of each reaction to the normalized intensity detected for protoplasts transfected with TGMV A replicon DNA and the empty expression cassette pMON921.

Sequence alignments. For each experimental database, the amino acid content of the 20-mer peptides was computed using a script, aminocounter.pl, that was coded using BioPerl modules (78). Based on this information, 100 random databases of equivalent sizes and contents were generated using the Perl script ranPEP.pl. The random and experimental peptide databases were formatted using NCBI formatdb.exe, and pairwise alignments were performed using the NCBI Basic Alignment Search Tool (BLASTP 2.2.10) (3) with a modified BLOSUM62 matrix (35). The modified matrix removed the stringent gap restriction and included similarities based on amino acid hydrophobicity and charge. An E value of 20 (scores of 10 bits or more) was used as the cutoff for the alignments, which were recorded as the number of peptides with hits and the sum of hits for all 20-mer peptides in each database. These frequencies were used to calculate the expected or observed mean and the standard error of the mean for each database, which were compared in one-way *t* tests using JMP 5.1 (SAS). The pairwise alignments of the experimental databases were further analyzed using the Vector NTI AlignX module (Invitrogen) to identify potential consensus motifs.

RESULTS

Yeast two-hybrid screens. Geminivirus replication proteins contain several conserved motifs that are essential for function. To develop new approaches to study and modulate these proteins, we screened the pJM-1 library for interacting peptides using the well-characterized TGMV replication protein designated here as TAL1. The pJM-1 library encodes *E. coli* thioredoxin (TrxA) with 2.9×10^9 random 20-mer peptides in its active site (18). The TrxA peptides are fused to the simian virus 40 nuclear localization signal, the *E. coli* B42 activation domain (AD), and the hemagglutinin epitope tag and are expressed from the yeast Gal1 promoter (18). For the screens, we constructed two types of TAL1 bait plasmids (Fig. 1A). $TAL1_{1\text{-}352}$ encodes the full-length TAL1 protein fused to the *E. coli* LexA DNA binding domain (DBD). $TAL1_{1\text{-}130}$ specifies a LexA DBD fusion with the first 130 amino acids of TAL1, which includes the conserved motifs I, II, and III (Fig. 1A). We also made a bait ($CaAL1_{1\text{-}349}$) containing the LexA DBD fused to the full-length coding sequence of the CaLCuV replication

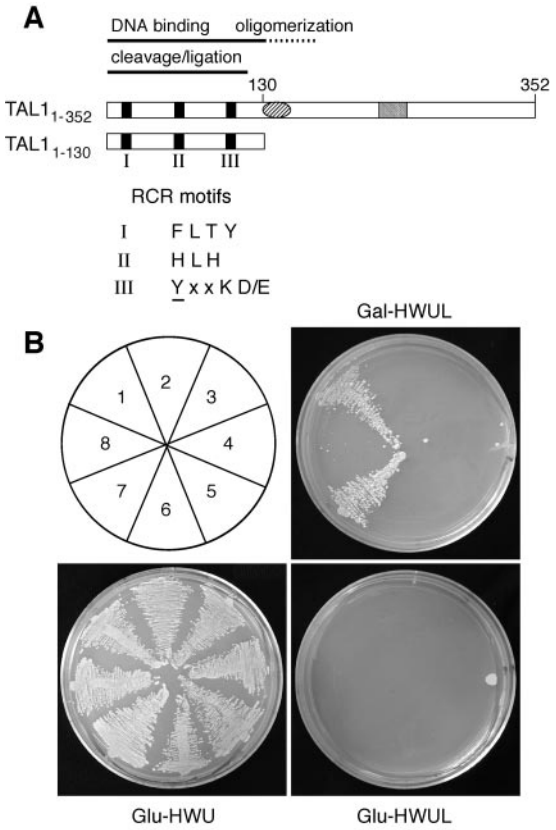

FIG. 1. Baits for aptamer screens. (A) Diagrams of the TGMV AL1 coding regions ($TAL1_{1-352}$ and $TAL1_{1-130}$) cloned downstream of the LexA DBD are shown. Motifs I, II, and III, which are associated with rolling-circle replication initiator proteins, are marked by the black boxes, and their consensuses are shown (39, 43). The oval corresponds to a conserved helix-loop-helix motif, and the gray box is the ATP binding motif. (B) Baits were tested for oligomerization activity using the positive (AD:$TAL1_{1-352}$) and the negative (AD:Jun) prey controls. The yeast transformants are $TAL1_{1-352}$ plus AD:$TAL1_{1-352}$ (1), $TAL1_{1-352}$ plus AD:Jun (2), $TAL1_{1-130}$ plus AD:$TAL1_{1-352}$ (3), $TAL1_{1-130}$ plus AD:Jun (4), GUS plus AD:$TAL1_{1-352}$ (5), GUS plus AD:Jun (6), $CaAL1_{1-349}$ plus AD:$TAL1_{1-352}$ (7), and $CaAL1_{1-349}$ plus AD:Jun (8). Interaction was monitored by growth on Gal−HWUL medium. Growth on Glu−HWU medium controlled for plasmid selection, whereas no growth on Glu−HWUL verified that the interaction is dependent on the induction of prey plasmid expression.

protein, designated here as CaAL1. We used GUS encoding a DBD:β-glucuronidase fusion as a negative control.

We took advantage of the oligomerization properties of TAL1 (61) to test the functionality of our full-length AL1 baits (Fig. 1). Yeast carrying the $TAL1_{1-352}$ bait and AD:$TAL1_{1-352}$ prey plasmids were able to activate the Leu reporter in the presence of galactose (Gal−HWUL plates) (Fig. 1B, area 1), consistent with the ability of full-length TAL1 to form oligomers. Transformants carrying the $CaAL1_{1-349}$ bait and AD:$TAL1_{1-352}$ prey plasmids also grew (Fig. 1B, area 7), indicating that the heterologous CaAL1 protein is able to interact with TAL1. In contrast, no growth was observed for the $TAL1_{1-130}$ bait (Fig. 1B, area 3), which lacks the oligomerization domain (62), or the GUS bait (Fig. 1B, area 5) in cotransfection assays with the AD:$TAL1_{1-352}$ prey plasmid. None of the baits interacted with the AD:Jun (Fig. 1B, areas 2, 4, 6, and 8) or the AD:TrxA-GST (data not shown) prey plasmids. All of the bait/prey combinations also failed to grow on selective medium supplemented with glucose (Glu−HWUL plates) (Fig. 1B). The presence of the bait and prey plasmids in the transformants was verified by growth on Glu−HWU plates. Similar results were obtained when activation of the *lacZ* reporter was used to detect interactions (data not shown). Together, these data established the specificity of the $TAL1_{1-352}$ and $CaAL1_{1-349}$ interactions. These results also verified that the interaction is dependent on galactose induction of prey plasmid expression and that none of the bait plasmids autoactivate the yeast reporters.

A two-step transformation protocol was used for the two-hybrid screens of the pJM-1 library (26). The yeast strain EGY48 was first cotransformed with the *lacZ* reporter pSH18-34 and the $TAL1_{1-352}$ bait plasmid. The recovered bait strains were transformed with 50 μg of library DNA. A total of 5×10^6 colonies were plated onto selective medium (Gal−HWUL) in two transformation events, resulting in the recovery of 350 colonies. These colonies were transferred onto Glu−HWU plates, grown for 2 days to repress library expression, and reevaluated for induction of the Leu and *lacZ* reporters on HWUL and HWU media supplemented with either galactose or glucose. Prey plasmids were recovered from 350 colonies that grew only in the presence of galactose. Retransformation assays using bait strains carrying $TAL1_{1-352}$ or GUS verified the specificity of interaction for 170 of the recovered plasmids, 40 of which were sequenced. Eleven TrxA peptides with unique sequences and no stop codons or frameshifts were selected for further analysis (Table 3).

To facilitate the identification of TrxA peptides that inhibit the essential DNA binding and cleavage activities mediated by the N terminus of AL1 (62), we also screened the pJM-1 library with the $TAL1_{1-130}$ bait (Fig. 1A). The screens were performed as described above for the $TAL1_{1-352}$ bait, except for the use of the stringent yeast strain EGY191 to ensure the identification of high-affinity interactions (28). In this experiment, 597 positive candidates were isolated from a screen of 2×10^7 yeast colonies. Interaction with $TAL1_{1-130}$ was confirmed for 287 yeast colonies displaying activation of both the Leu and *lacZ* reporters. Prey plasmids were recovered and sequenced for 130 colonies, out of which 88 unique TrxA peptides were selected (Table 4).

TABLE 3. Aptamers isolated in screens with $TAL1_{1-352}$

Aptamer	Peptide sequence	Yeast plasmid[a]	Expression cassette[b]
FL-1	PLSGRQGVHLYFLLLMPA	B1118-001	pNSB1138
FL-7	FAVEYGSQGWGLWYCVWLDL	B1118-007	pNSB1141
FL-18	FQSRMGGGSGVVNAKLWAKE	B1118-018	pNSB1137
FL-19	VASRDSGAWRELHSFLNFAS	B1118-019	pNSB1135
FL-41	YYMALLYSQCPTVVLFRMTT	B1118-041	pNSB1139
FL-42	DFVCLCLFACTSDLSAFRVC	B1118-042	pNSB1136
FL-57	TAFRWDMFWMHTSGTWRKP	B1118-057	pNSB1143
FL-60	FASGSGEPVGLGLGSPLEKL	B1118-060	pNSB1144
FL-70	VYDSALCLVVGRCGLIRCR	B1118-070	pNSB1134
FL-90	LVWASM	B1118-090	pNSB1142
FL-99	LHESCWGWAGDSSPQGVLAG	B1118-099	pNSB1140

[a] The yeast plasmids were cloned into pJM-1 with carbenicillin selection.
[b] The plant expression cassettes were cloned into pMON921 with carbenicillin selection.

TABLE 4. Aptamers isolated in screens with $TAL1_{1-130}$

Aptamer	Peptide sequence	Yeast plasmid[a]	Expression cassette[b]	Aptamer	Peptide sequence	Yeast plasmid[a]	Expression cassette[b]
A-3	GFRAPGLSPTRPSCLICSTL	B1162-3	pNSB1228	A-114	VRSHRRYQRNWEPVVSWFSS	B1162-114	pNSB1279
A-5	NECLICHMLGIREFGLSA	B1162-5	pNSB1229	A-115	WCGPQVSARCK	B1162-115	pNSB1253
A-6	GTLWRRCASSWAFPPDCPSA	B1162-6	pNSB1230	A-116	SCDEAFDAASVASELFCQPY	B1162-116	pNSB1280
A-8	RRALRHCTGCMLSQRLGTAL	B1162-8	pNSB1258	A-117	ARMALSLREWEYLFFKDAPSGPGL QGLSLASRLNLVILRGYG	B1162-117	pNSB1228
A-9	HSMHSCSVGRCLVDVKVVVS	B1162-9	pNSB1231				
A-12	WMVCAGCGALRTRQVTLHPG	B1162-12	pNSB1232	A-119	RSYGGGEIPSVTMHCWIHCD	B1162-119	pNSB1281
A-15	GGFVPMRLCTCLLIVRLFI	B1162-15	pNSB1264	A-123	SSSRWVPFALQDPLFSSDDW	B1162-123	pNSB1282
A-16	VPQPLNCDLCVLMGGASSSR	B1162-16	pNSB1233	A-124	YLWSSKMDEWVAMDDVYAAC	B1162-124	pNSB1283
A-18	RRDYRKFFALNCQLCRLTVT	B1162-18	pNSB1234	A-127	TWGLVCTGTGWGLLDTVVRA	B1162-127	pNSB1284
A-22	CRTRGCGCHLCRMLSQFTGG	B1162-22	pNSB1235	A-129	VYEWGDVLCGGSMAIQWGL	B1162-129	pNSB1254
A-25	MRLGKGWNLMFLEEVSVLDA	B1162-25	pNSB1323	A-130	ASNGEIAYCVEQAMLLLCFH	B1162-130	pNSB1285
A-27	RDPQLGQVAQTWGCRLCLLE	B1162-27	pNSB1259	A-131	ELIVHEWPLILSRVGRIVL	B1162-131	pNSB1255
A-30	LVSESCGSWFCLCPWEVLNW	B1162-30	pNSB1263	A-132	GRVQLEILVSEAEEGVSPFL	B1162-132	pNSB1286
A-40	LQYSWNLYSVASFKTRRVSS	B1162-40	pNSB1236	A-135	RDAEWQDVLGRARAVHLRGR	B1162-135	pNSB1287
A-41	RLQESSIDLTPGIYLGMDFV	B1162-41	pNSB1265	A-136	GLKWKSDNGCVYVSFMRGGV	B1162-136	pNSB1288
A-46	CYMEVEGRPRRWADSFFVAW	B1162-46	pNSB1262	A-137	SSSPVPYSGGTCNLCSMRMW	B1162-137	pNSB1289
A-49	SESFVCKTCHMLRVSDAVGA	B1162-49	pNSB1260	A-140	EWEDPQYAGWELFSISDLVH	B1162-140	pNSB1256
A-50	MHVSLVFPWRLTGHIQQYKV	B1162-50	pNSB1261	A-141	PMVRTEWPLCAIIPLSMLYQ	B1162-141	pNSB1290
A-51	GRCNLQGMSFMGVGRSVWFE	B1162-51	pNSB1237	A-143	RAGWHERVRQWWAIECTLEV	B1162-143	pNSB1291
A-53	VVGGSLRDEWKWWREGRSLP	B1162-53	pNSB1267	A-145	SVRCWYVLRCSFLVGSGSSV	B1162-145	pNSB1292
A-59	AKDVERGAGGKIKACELCRL	B1162-59	pNSB1268	A-146	RSCVLCAYGSRTFNGSYLLF	B1162-146	pNSB1257
A-63	VETFKARARQTPSCDLCPKT	B1162-63	pNSB1238	A-147	GRGGCMLCDVDGSSAWLHTEGRLT GPITSQQCLSFQYLGNGEFIDG	B1162-147	pNSB1266
A-64	TELWWADFAKMHMEGGKGMC	B1162-64	pNSB1239				
A-67	RHRCTSRAPRQWFRPHRDSP	B1162-67	pNSB1269	A-149	TLETLDMGNPLYTCVLMDWM	B1162-149	pNSB1324
A-69	RYRVSAGPLCSLCSLWGSVG	B1162-69	pNSB1240	A-150	LVMGWRSEVSSLQGKTGTGGGPTL RKCQLCRGSRYTLKYYPC	B1162-150	pNSB1293
A-71	EEGLAAITHTWLTMCFAAGL	B1162-71	pNSB1241				
A-73	AAFLESVRSYWSRFVRHVQG	B1162-73	pNSB1242	A-153	RPGCPFCTSWRCG	B1162-153	pNSB1294
A-75	RAMCDKDKSVCSILALYVQV	B1162-75	pNSB1243	A-155	FCPECQMVAGAEDGDAIDLQ	B1162-155	pNSB1295
A-80	CWWLREIGTFRCVTLQHVAG	B1162-80	pNSB1244	A-158	RRCMLCTSDKPGGDQGALNM	B1162-158	pNSB1296
A-82	FESAWSTLMGAMTPMVLDET	B1162-82	pNSB1270	A-159	LWGGGTAWDFFVWGEDSAC	B1162-159	pNSB1297
A-83	QALVVSPETFLCLEALGVNS	B1162-83	pNSB1271	A-160	GMSGRIPEPDDWVVLFITGC	B1162-160	pNSB1298
A-84	GGRQTEPSLTLLADLTLLLS	B1162-84	pNSB1272	A-161	GGTNALLQKVFFGEVGVASM	B1162-161	pNSB1299
A-86	GSRAELSAPEVAWLLFCTPG	B1162-86	pNSB1245	A-164	ECCLFPIFAMADSFPCPSPV	B1162-164	pNSB1300
A-87	RYSAVCRDCYEGHGRGLWYM	B1162-87	pNSB1273	A-165	MLEGPLDQGLMMGTCCWECS	B1162-165	pNSB1301
A-89	GGWLVTIVEGPLAICCLRDD	B1162-89	pNSB1274	A-166	TPSVTWLAEWCSCVFCRDAS	B1162-166	pNSB1302
A-90	PSIESGWVGDQAVAPCDLSV	B1162-90	pNSB1275	A-167	SWWWANNSLCREWEFAC	B1162-167	pNSB1303
A-91	TWGAWKRDIVLVSEIGFTWG	B1162-91	pNSB1246	A-168	WNMLAFGGALVASGLLRGWE	B1162-168	pNSB1304
A-94	RLGGGRPKLWHFSPNLMAGF	B1162-94	pNSB1247	A-169	DKCDDVEPFLWWGQQCFFDV	B1162-169	pNSB1305
A-97	ERVHVCFSRKCTALSVDSSV	B1162-97	pNSB1248	A-170	GSPSRISYTCLSPDVTLLFL	B1162-170	pNSB1306
A-99	RERGGDDYRRMMHPGAASGP	B1162-99	pNSB1249	A-172	MGIEACSITECTSQHCNEVA	B1162-172	pNSB1307
A-100	RLVVGCEWRIGCSTGSGPRG	B1162-100	pNSB1250	A-173	CLDNLCWELGGGFPVILIHC	B1162-173	pNSB1308
A-101	ASLIGVGIASMHGMQTDGIY	B1162-101	pNSB1251	A-174	HVHGSCPSMGWSSNSWCSVF	B1162-174	pNSB1309
A-108	VGLMEWAVWSLEVREKLYSC	B1162-108	pNSB1276	A-175	PLELEFAVCGCSWLVALDWS	B1162-175	pNSB1310
A-109	VLGRLGGAGGCSLCDQLEAL	B1162-109	pNSB1277	A-176	AWDSESLATWASVMPWPYPT	B1162-176	pNSB1311
A-110	IWINPNGLWWTKVGLNPYAV	B1162-110	pNSB1252	A-177	TGCHYKGARCCRLTWDVLIL	B1162-177	pNSB1312
A-112	RHESALHKSCELCYCPWKVC	B1162-112	pNSB1278				

[a] The yeast plasmids were cloned into pJM-1 with carbenicillin selection.
[b] The plant expression cassettes were cloned into pNSB1226 with kanamycin selection.

Because these TrxA peptides were selected for binding to a truncated TAL1 protein that does not oligomerize, we asked if they also interact with full-length TAL1. Figure 2B shows that yeast cotransformed with each of the 88 TrxA peptides in the presence of either $TAL1_{1-130}$ or $TAL1_{1-352}$ baits grew in Gal−HWUL medium. Cotransfection with the negative-control bait GUS did not induce the Leu reporter, and no growth occurred (Fig. 2B). No growth was seen on plates lacking leucine but supplemented with glucose (Fig. 2C). Growth on Glu−HWU medium confirmed the presence of the prey and bait plasmids in all of the transfections (Fig. 2D). Based on these results, we concluded that the 88 TrxA peptides initially selected for interaction with $TAL1_{1-130}$ also bind to $TAL1_{1-352}$.

TrxA peptides that bind to TGMV AL1 interfere with viral DNA replication. We asked if binding of the TrxA peptides impacts TAL1 function during viral replication. The 11 FL-TrxA peptides (Table 3) selected in the screen using the $TAL1_{1-352}$ bait were subcloned into a plant expression cassette containing the CaMV35S promoter with a duplicated enhancer and the *rbcS* E9 terminator. The constructs were cotransfected into tobacco protoplasts in the presence of a replicon plasmid containing a partial tandem copy of TGMV A that supports the release of unit-length viral DNA (Fig. 3A). TGMV A DNA, which encodes TAL1 and its replication accessory factor, AL3 (Fig. 3A), replicates autonomously and accumulates to a high copy number in plant cells (59). We asked if expression of the full-length TrxA (FL-TrxA) peptides quantitatively impacts TGMV A DNA accumulation as an indicator of altered TAL1 activity. Total DNA was isolated 48 h posttransfection, and the levels of double-stranded TGMV A DNA were examined by DNA gel blot hybridization. Nine of the FL-TrxA peptides had no detectable effect on viral DNA accumulation (data not shown). In contrast, cells containing the FL-42 (Fig. 3B, lane 3) and FL-60 (lane 4) cassettes accumulated to only about 25% of the levels detected in a transfection containing an empty expression cassette (lane 2). The level of viral DNA detected in the presence of FL-42 and FL-60 was similar to that seen for FQ118 (Fig. 3B, lane 1), a strong

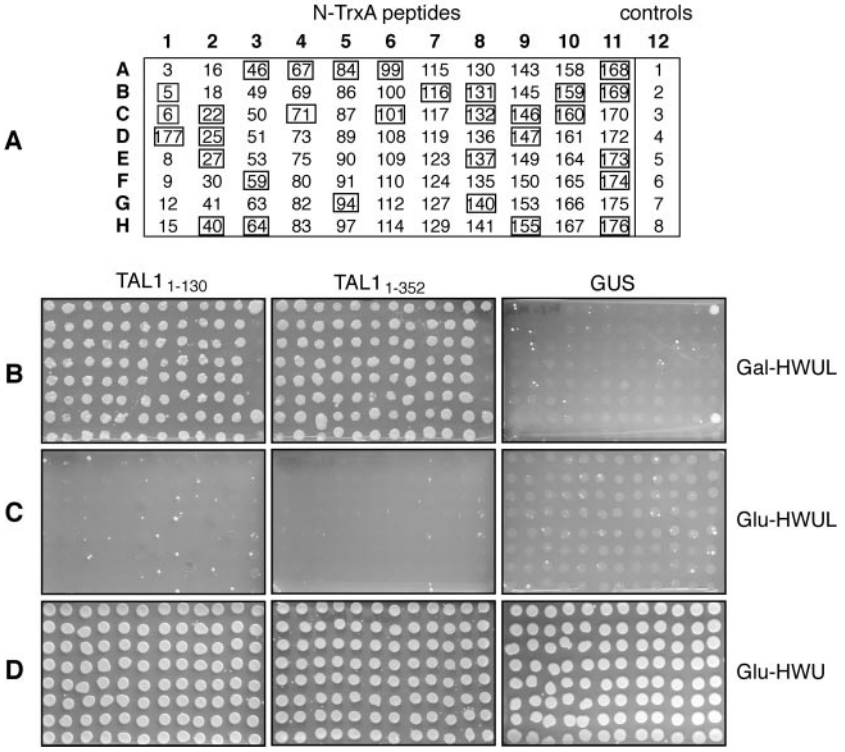

FIG. 2. Aptamers that bind to $TAL1_{1-130}$ also interact with $TAL1_{1-352}$. The 88 plasmids recovered from the screen of the JM-1 library using $TAL1_{1-130}$ as bait were retransformed into different bait strains to confirm the specificity of the interaction. (A) Key for N-TrxA peptides on the plates in B to D. Controls in column 12 are numbered as described in the legend of Fig. 1. The interaction assay was performed on Gal−HWUL (B), Glu−HWUL (C), and Glu−HWU (D) media with the $TAL1_{1-130}$, $TAL1_{1-352}$, and GUS baits, as indicated at the top. Peptides that interfere with the replication of TGMV are boxed in A.

trans-dominant-negative mutant of TAL1 (61). These results indicated that two of the FL-TrxA peptides interfere with the ability of TAL1 to support viral DNA replication.

The 88 N-TrxA peptides were also tested in replication interference assays. For these experiments, we used a semiquantitative PCR protocol to facilitate the analysis of a large number of expression cassettes (33). The assay is based on primers that distinguish the input replicon cassette and nascent viral DNA by size and DpnI sensitivity. Primers LLp1 and LLp2 (Table 2 and Fig. 3A) amplify a 4.9-kb DNA from the replicon cassette and a 1.2-kb product from the released TGMV A component (Fig. 3C, lane 1) in DNA extracts from *E. coli* cells carrying the replicon cassette plasmid. Even though the replicon cassette is the prevalent form in *E. coli* (data not shown), it amplified less efficiently than the released TGMV component because of its large size. The production of both products is sensitive to DpnI digestion (Fig. 3C, lane 2) and resistant to MboI digestion (lane 3), indicative of an *E. coli* Dam-methylated template. Interestingly, the same results (Fig. 3C, lanes 4 to 6) were obtained for the mutant TGMV A replicon cassette with a frameshift mutation at TAL1 amino acid position 120 (21).

The amplification strategy was also tested with DNA extracted from tobacco cells cotransfected with various TGMV A replicon and expression cassettes. We first asked if the input and nascent viral DNA can be distinguished by comparing DNA samples isolated from cells transfected with the wild-type TGMV A replicon cassette or the mutant AL1 cassette. The 1.2-kb product (Fig. 3D, top band) was produced when uncut and MboI-digested DNA from cells transfected with both cassettes was amplified (Fig. 3D, lanes 1 to 3 and 10 to 12, top and bottom). In contrast, the 1.2-kb product was amplified only from DpnI-treated DNA from cells with the wild-type cassette (Fig. 3D, lanes 1 to 3, middle) but not the mutant cassette (lanes 10 to 12, middle). This result demonstrates that residual Dam-methylated *E. coli* DNA can be quantitatively removed by DpnI digestion, thereby allowing the detection of nascent DNA by PCR. We then verified that replication interference can be monitored by PCR by showing that the level of the 1.2-kb PCR product is reduced in cells carrying a TAL1 dominant-negative mutant (FQ118) expression cassette (Fig. 3D, lanes 7 to 9) relative to cells with the empty (lanes 1 to 3) or TrxA-GST (lanes 7 to 9) cassettes. This difference was not apparent in uncut or MboI-treated DNA because of the presence of intact *E. coli* input DNA (Fig. 3D, lanes 1 to 9, top and bottom). Similar results were seen for the three biological replicas for each transfection condition. Together, these results established that the PCR assay can be used to monitor viral DNA accumulation in a reproducible, semiquantitative manner.

Expression cassettes corresponding to the 88 N-TrxA peptides (Table 4) were transfected into tobacco protoplasts with the wild-type TGMV A replicon cassette. Total DNA was isolated 36 h after transfection and analyzed in replication

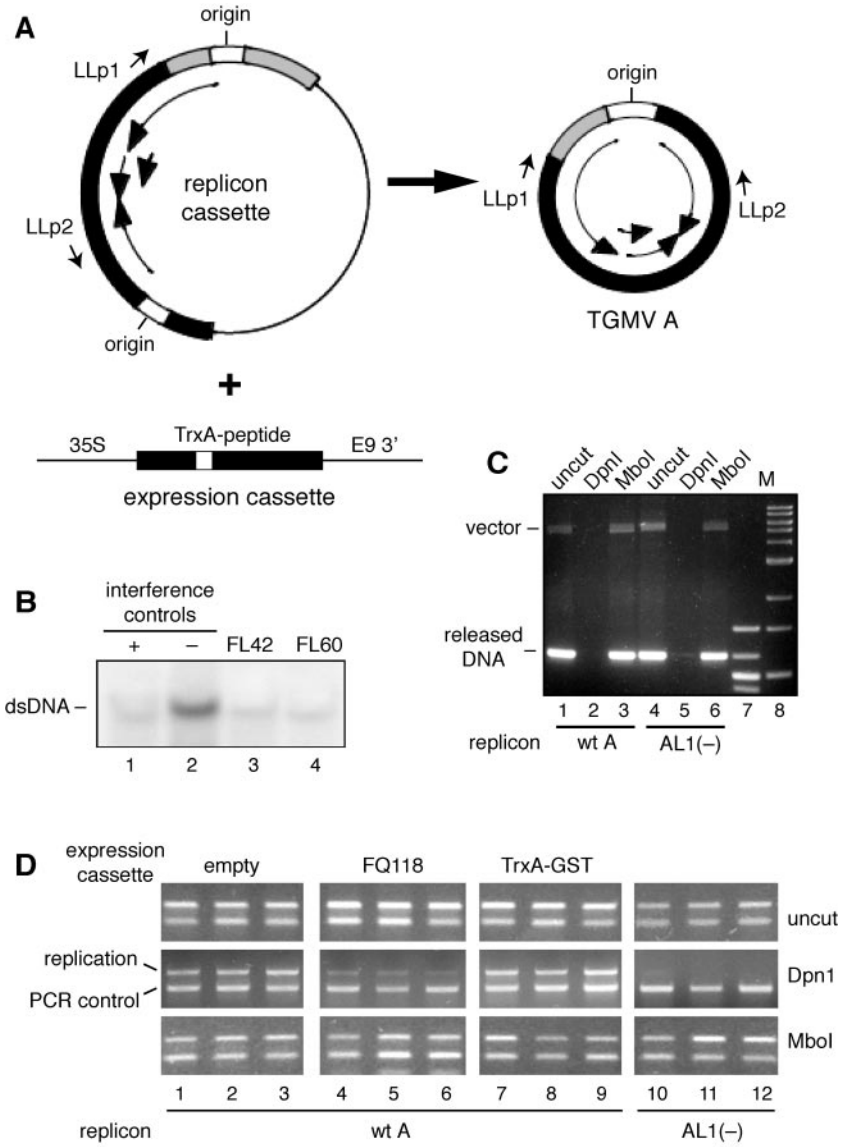

FIG. 3. Replication interference assays. (A) The diagram shows the input replicon cassette, the released TGMV A replicon, and the plant expression cassettes. The positions of primers (LLp1 and LLp2) used to distinguish input vector and replicated DNA are marked. (B) Tobacco protoplasts were cotransfected with a TGMV A replicon (pMON1565) (lanes 1 to 4) and a plant expression cassette. Total DNA was isolated 36 h posttransfection, digested with DpnI and XhoI, and analyzed on DNA gel blots using a virus-specific probe for double-stranded DNA accumulation (dsDNA). The expression cassettes correspond to the *trans*-dominant TAL1 mutant FQ118 (pNSB866) (lane 1), an empty cassette (pMON921) (lane2), aptamer FL-42 (pNSB1136) (lane 3), and aptamer FL-60 (pNSB1144) (lane 4). (C) Released DNA can be amplified from *E. coli* cells transfected with an AL1 mutant replicon cassette. Total DNA was isolated from *E. coli* cells transformed with either a wild-type (wt) TGMV A replicon cassette (pMON1565) (lanes 1 to 3) or a mutant replicon cassette carrying an AL1 frameshift mutation (pMON1679) [AL1(−), lanes 4 to 6] and amplified using primers LLp1 and LLp2 (A). These primers did not amplify a product in reaction mixtures containing pUC18, the cloning vector used to construct pMON1565 (data not shown). The methylation status of the template DNAs was assessed by digestion with DpnI (lanes 2 and 5) and MboI (lanes 3 and 6). PCR products corresponding to the replicon cassette and released TGMV A DNA are marked. Markers corresponding to 100-bp (lane 7) and 1-kb (lane 8) DNA ladders are shown. (D) TGMV A replication requires full-length AL1 in plant cells. Tobacco protoplasts were transfected with a wild-type TGMV A replicon (pMON1565) (lanes 1 to 9) or the mutant AL1 replicon cassette (pMON1679) (lanes 10 to 12). In lanes 1 to 9, plant expression cassettes corresponding to an empty cassette (pMON921) (lanes 1 to 3), the *trans*-dominant AL1 mutant FQ118 (pNSB866) (lanes 4 to 6), and the TrxA-GST control (pNSB1166) (lanes 7 to 9) were included in the transfections. Total DNA was isolated 36 h posttransfection and analyzed directly by PCR or after digestion with DpnI or MboI.

interference assays using the semiquantitative PCR method. Because of the high number of samples, the N-TrxA peptides were initially analyzed in triplicate in three separate experiments. We selected 35 N-TrxA peptide cassettes that reduced viral DNA accumulation relative to the empty expression cassette. The selected cassettes were then assayed in a single transfection experiment (Fig. 4), with 31 of 35 cassettes showing statistically significant interference activity ($P < 0.05$ in a one-tailed Students t test). The experiment also included the FQ118 and TrxA-GST expression cassettes as positive and

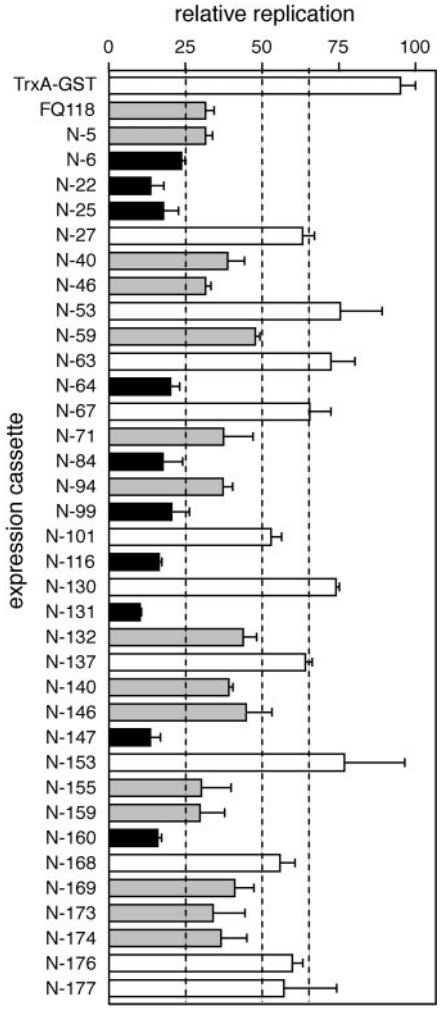

FIG. 4. Some aptamers that bind to $TAL1_{1-130}$ interfere with TGMV replication. The N-TrxA peptides selected by screening with $TAL1_{1-130}$ and cloned into plant expression cassettes (Table 4) were tested in replication interference assays using the semiquantitative PCR assay shown in Fig. 3D. Bands corresponding to the replicated TGMV A DNA (1.2 kb) and the PCR internal control (700 bp) were quantified using ImageJ software (1, 66). Replication in the presence of the expression cassettes indicated on the left was normalized to amount of replicated DNA in the presence of the empty expression cassette (set to 100). Cutoff values of ≥25%, ≥50%, and ≥65% indicate strong (black bars), moderate (gray bars), and weak (white bars) interference, respectively. Some N-TrxA peptides show no significant interference (also in white bars). Each assay was performed in triplicate, with the error bars corresponding to 2 standard errors.

negative controls, respectively. The N-TrxA peptides were classified as weak (50 to 65%), moderate (25 to 50%), and strong (<25%) interferers (Fig. 4, dotted lines) relative to the control transfection with an empty cassette (100%). Ten N-TrxA peptides showed strong interference (Fig. 4, black bars), 14 exhibited moderate interference (gray bars), and seven were weak interferers (white bars). In total, 14 aptamers displayed interference activity that was greater or equal to that of FQ118. TrxA-GST did not impact viral DNA accumulation, indicating that the TrxA sequences per se do not contribute to interference.

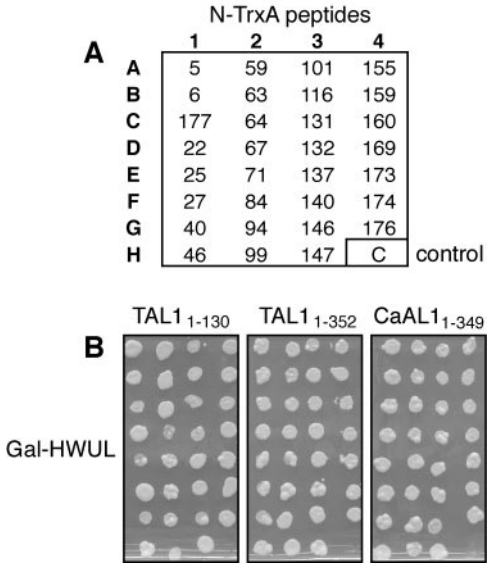

FIG. 5. Aptamers interact with AL1 from a heterologous geminivirus. Selected N-TrxA peptides were tested for interaction with CaLCuV AL1. (A) Key for the aptamers on the plates in B. The negative prey control, AD:Jun, is marked by a "C." (B) Yeast cells containing the selected aptamers and the $TAL1_{1-130}$ (left), $TAL1_{1-352}$ (center), and $CaAL1_{1-349}$ (right) baits were analyzed for growth on Gal−HWUL medium.

N-TrxA peptides also interact with CaAL1. Motifs I, II, and III in $TAL1_{1-130}$ (Fig. 1A) are conserved in all geminivirus replication proteins (39, 43). Hence, we asked if peptides that bind to $TAL1_{1-130}$ and inhibit TGMV replication are also able to interact with an AL1 protein from a heterologous geminivirus. For this experiment, we chose the CaLCuV AL1 protein because it shares only 42% identity and 58% similarity with TAL1 across the first 130 amino acids. Full-length CaAL1 fused to the LexA DBD ($CaAL1_{1-349}$) was used as bait in yeast two-hybrid assays with the 31 N-TrxA peptides that displayed replication interference activity (Fig. 4). All of the peptides were positive for interaction with $CaAL1_{1-349}$ in growth assays (Fig. 5B, right). The prey control did not interact with any of the baits (Fig. 5).

Pairwise alignments of the N-TrxA peptides. We asked if the 20-mer inserts in the N-TrxA peptides are random or related because of their selection for binding to $TAL1_{1-130}$. The 20-mer peptides were grouped into three database corresponding to the 88 peptides selected for binding to $TAL1_{1-130}$ ("all"), the 31 peptides positive for replication interference ("interfering"), and the 57 peptides negative for interference ("noninterfering"), and their sequences were compared in pairwise alignments using BLASTP. The score values of the alignments were low (data not shown) because of the short length of the peptide sequences (20 amino acids). To address the possibility that the alignments were produced by chance, 100 sets of three random databases of the same size and amino acid content as the N-TrxA peptide were compared using BLASTP. The distribution of the frequency of hits was analyzed for each database and used to determine the expected mean and standard error of the mean for random sequences.

The frequency distribution of the 100 databases comprising the 88 random 20-mer peptides is shown in Fig. 6A. The left

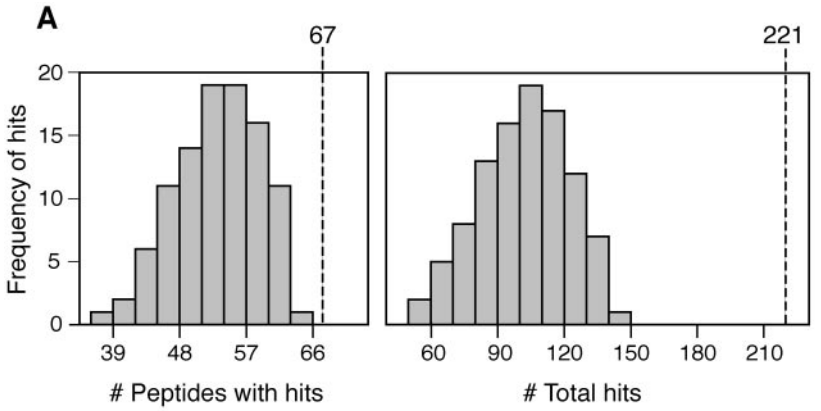

B

	# Peptides with hits		#Total hits	
	Observed	Expected ± SE	Observed	Expected ± SE
All	67	54 ± 0.57	221	101 ± 0.2
Interfering	18	11 ± 0.38	40	14 ± 0.69
Non-interfering	36	28 ± 0.5	74	43 ± 0.14

FIG. 6. Statistical significance of pairwise alignments. Pairwise alignments were performed for 100 sets of three random databases of computer-generated 20-mer aptamers containing 88, 31, or 57 members. The frequencies of hits were compared to equivalent alignments of the databases corresponding to all, interfering, and noninterfering N-TrxA peptide databases, respectively. (A) The left panel shows the frequency distribution (expected mean, 54) of a random 20-mer peptide having at least one hit against a database comprised of 88 random 20-mer peptides. The right panel shows the frequency distribution (expected mean, 101) of the total number of hits per peptide for all the 88 random 20-mer peptides. The dashed lines represent the observed values for the all N-TrxA peptide database for each analysis. Similar analyses were performed for the interfering and noninterfering TrxA peptide databases and their random 20-mer control databases (not shown). (B) The observed and expected means and standard errors of the pairwise alignments of the three TrxA peptide databases are given. The observed values for the three databases are significantly higher than the expected values derived from the random 20-mer databases (P values of <0.0001).

panel represents the expected distribution of peptides with at least one hit, while the right panel shows the frequency distribution of the total number of hits for all the 20-mer peptides in the database. The expected means of the two distributions (54 and 101, respectively) are lower than the observed means (67 and 221, respectively) for the all database (Fig. 6B). The observed means for the interfering and noninterfering databases are also higher than the expected means calculated using the corresponding random databases (Fig. 6B). The observed and expected means of all three databases differed by at least 2 standard deviations and gave a P value of <0.0001 in one-way Student's t tests. These results established that even though N-TrxA peptides were derived from a random library, their sequences are not random.

Inspection of the BLASTP alignments revealed that some pairs contained common sequences. Similar pairs were grouped and compared using the Vector NTI AlignX module. A total of 18 groups containing four or more sequences were identified among the 88 N-TrxA peptides. The putative motifs were filtered using four criteria: (i) motifs include at least five members, (ii) members interact with CaAL1, (iii) motifs contain amino acids typically involved in protein-protein interactions (7, 27), and (iv) motifs are related to a plant protein. Seven motifs that satisfied at least three criteria are shown in Fig. 7A. (The sequence alignments are shown in Fig. S1 and S2 in the supplemental material.) Motifs 1, 4, 20, 25, and 27 consist primarily of interfering peptides, while motif 28 is composed of mostly noninterfering peptides. Motif 24 includes 18 members that are distributed between interfering and noninterfering peptides, all of which contain a core CxLC sequence (Fig. 7B). The interfering members also include conserved polar and nonpolar residues flanking the core sequence (see Fig. S1 in the supplemental material). These residues occur individually in noninterfering peptides, but only the interfering peptides contain both sets of flanking residues.

DISCUSSION

Peptide aptamers are recombinant sequences that have been selected for specific binding to a target protein in screens of combinatorial libraries (37). They have been used to interfere with protein function in bacterial, yeast, and animal systems (19). Their ability to interact with viral proteins and act as antiviral agents has been demonstrated in animal cells (10, 67). In plants, peptide aptamers and the related scFv antibodies have been effective against RNA viruses (8, 65, 81). In this report, we identified peptide aptamers that target a geminivirus replication protein and interfere with its function in vivo. This research represents the first example of peptide aptamers that inhibit the replication of a plant DNA virus and supports the possibility of using aptamer technology to develop broad-based resistance against geminivirus disease in crops.

To examine the impact of TrxA peptides on geminivirus replication in plant cells, we used a high-throughput assay

A

Sequence	All	Interfering
WxDx_3A**W**	6	4
MHx_5G	6	5
$\frac{L}{M}$ G**G**x_2P	8	5
$\frac{G}{S}$ **C**xL**C**xL	18	7
Wx_3**S**LC	6	5
$\frac{S}{A}$Fx_2AxV**A**S	7	6
WGX**V**L	5	1

B

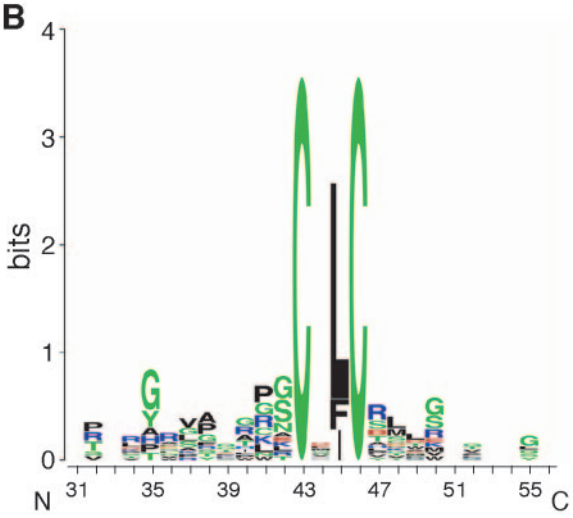

FIG. 7. Motifs involved in AL1 binding and replication interference. (A) Consensus sequences corresponding to motifs identified in pairwise alignments of the 88 TrxA peptides. Boldface type indicates invariant residues, normal typeface marks amino acids conserved in a majority of group members, and x represents any amino acid. The number of members and interfering peptides in each group are listed on the right. (See Fig. S1 and S2 in the supplemental material for sequence alignments.) (B) WebLogo representation of motif 24. The amino acid type and position are shown on the *x* axis. The overall height of the amino acid stacks, plotted on the *y* axis, indicates the sequence conservation at a given position, while the height of individual symbols within a stack indicates the relative frequency of an amino acid at that position (20, 72). Amino acids are color coded according to their type as basic (blue), hydrophobic (black), polar/nonpolar (green), and acidic (red) (7, 27).

based on semiquantitative PCR to measure viral DNA accumulation. PCR-based strategies have been used to monitor DNA virus loads in animal and plant systems (33, 52, 77). This assay relies on the methylation status of the DNA template and the size of the PCR product to discriminate between the input replicon cassette DNA and de novo-replicated viral DNA in plant cells (Fig. 3D). Interestingly, our PCR primer pair detected a DpnI-sensitive product corresponding to released viral DNA in *E. coli* cells transformed with a wild-type TGMV A replicon cassette (Fig. 3C, lane 1) or a cassette that can express only the first 120 amino acids of AL1 (lane 4). This region of AL1 is sufficient for DNA cleavage and ligation in vitro but does not support viral DNA replication in plant cells (21, 62). Hence, previous reports of TGMV and other geminiviruses replicating in bacteria (68, 73) may reflect AL1-catalyzed release and ligation of unit-length viral DNA and not actual replication. If viral DNA replicates in *E. coli*, it is not dependent on a fully functional viral replication protein and is likely to occur via a different mechanism than that of plant cells.

We selected 88 peptide aptamers that bind to the TGMV AL1 N terminus, 31 of which interfere with TGMV replication in transient assays. Twenty-four peptide aptamers reduced viral replication by at least 50%, with 14 aptamers displaying similar or stronger interference activity compared to the FQ118 *trans*-dominant-negative AL1 mutant. The high frequency of strongly interfering peptides is striking. Peptide aptamers with constrained conformations can bind to their targets with 10^2- to 10^3-fold higher affinity than unconstrained peptides (26). A high proportion of interfering aptamers that bind to the rabies virus P protein were also selected in a screen of a conformationally constrained peptide library in yeast two-hybrid assays (67). Stringent in vivo screens also select for high-affinity aptamers that are correctly folded and stably expressed in an intracellular context. Hence, the large number of strongly interfering peptides isolated in the two studies probably reflects strong interactions between the target protein and the constrained peptides selected in vivo (26, 67). Another similarity between the two studies is the targeting of a low-abundance viral protein essential for replication and transcription, which is likely to be more sensitive to inactivation than a more abundant structural protein. Consistent with this idea, single-chain antibody experiments showed that viral RNA-dependent RNA polymerases are sensitive to depletion in transgenic plants (8).

Our screen using the full-length $TAL1_{1\text{-}352}$ bait identified 2 of 11 interfering peptides, compared to the 31 of 88 peptides in the screen using the truncated $TAL_{1\text{-}130}$ bait (e.g., 18% versus 35%). The apparent difference in efficiencies may reflect the accessibility of essential AL1 motifs in the two baits. Nuclear magnetic resonance spectroscopy of the N-terminal domain showed that motifs I, II, and III are exposed on a β-sheet surface (12) and may thus be more accessible for aptamer binding in a truncated AL1 protein. Interestingly, 29 of the 54 identical residues in the N termini of TAL1 and CaAL1 are located in motifs I, II, or III or are predicted to be exposed on the protein surface (12).

The interfering peptide aptamers could act through several distinct mechanisms. They might inhibit the DNA binding and cleavage/ligation activities catalyzed by the AL1 N terminus (60), compete for AL1/AL3 or AL1/pRBR binding between amino acids 101 and 180 (4, 42, 75), or block access to the protein interaction domain between residues 134 and 180 (61). Consistent with these possibilities, there are examples of peptide aptamers that inhibit transcription factor DNA binding activity (23, 56), block the catalytic activity of regulatory and signaling proteins (17, 71), and interfere with protein-protein interactions required for the assembly of viral replication complexes (10, 67).

A comparison of the overall amino acid composition of the N-TrxA peptides with different databases indicated that they are more similar to eukaryotic than to prokaryotic proteins (data not shown). The peptides are enriched for cysteine, glycine, and arginine, while lysine, isoleucine, and aspartic acid

are underrepresented. These amino acids frequently occur at protein interfaces and are involved in protein-protein interactions (27). In silico analysis demonstrated that the sequences of the N-TrxA peptides are not random and identified seven potential binding motifs (Fig. 7A). These motifs include 41 of the 88 peptides and 22 of the 31 interfering peptides (see Fig. S1 and S2 in the supplemental material). In addition, 12 of the excluded peptides contain sequences that resemble the seven motifs. These numbers indicate that even though our database is small, the seven motifs capture much of the similarity between the N-TrxA peptides. A random peptide screen uncovered three binding motifs that target distinct sites on the PCNA protein (83). Our results suggest that the AL1 N terminus also includes a limited number of binding targets. It is not possible to correlate a specific motif with replication interference. However, motifs 1, 4, 20, 25, and 27 are more highly represented in interfering peptides, while motif 28 is found primarily in noninterfering peptides (Fig. 7; see Fig. S1 and S2 in the supplemental material).

Motif 24 is the most highly represented motif, encompassing over 20% of the N-TrxA peptides. Given the large size of this group, its members are likely to target a hot spot on the surface of AL1. There is no correlation between the occurrence of motif 24 and replication interference activity, indicating that the core CxLC sequence is not sufficient for interference. Interfering members of motif 24 contain additional conserved residues adjacent to the core, which may enhance or alter contact with AL1 and result in interference. The idea that supplementary amino acid contacts are required for interference is also supported by the observation that some interfering aptamers include multiple motif sequences. These peptides fall into two classes: those with overlapping motifs and those with separable motifs. The first class is exemplified by N-40, N-140, and N-176, which include motifs 1 and 25, and by N-5 and N-22, which contain motifs 4 and 24. In these cases, the motifs have related sequences and may constitute an extended binding interface. The second class is demonstrated by N-176, which contains nonoverlapping motif 25 and motif 28 sequences, suggesting that it can target two different sites in AL1.

Several properties of the interfering N-TrxA peptides suggest that they can be used to develop geminivirus-resistant plants. First, they were isolated in a stringent in vivo screen and, as such, are likely to bind to AL1 with high affinity, fold correctly, and be stably expressed in a cellular environment. Second, they were selected for binding to the N terminus of AL1, which does not resemble plant proteins. As a consequence, the peptides are unlikely to interact with host proteins, minimizing the risk that their expression will be toxic to plants. Third, the N-TrxA peptides are ca. 12 kDa, a size typical of a small, stable protein that can move passively into the nucleus, where AL1 is localized. Fourth, several of the peptides reduce TGMV DNA accumulation more strongly than a *trans*-dominant-negative TAL1 mutant that can confer immunity to TGMV infection (M. Dallas and L. Hanley-Bowdoin, unpublished data) and a truncated C1 mutant that bestows tomato yellow leaf curl virus resistance (58) when expressed in transgenic *Nicotiana benthamiana* plants. Last, the ability of N-TrxA peptides to bind to the divergent TAL1 and CaAL1 proteins suggests that they recognize conserved features in the N termini of geminivirus replication proteins. This represents a key difference from interference strategies based on viral sequences like mutant viral proteins, antisense RNAs, and RNA interference constructs, all of which are effective only against the cognate geminivirus or closely related viruses. In contrast, a resistance strategy based on the interfering N-TrxA peptides could be broadly applicable to all geminivirus genera and other eukaryotic single-stranded DNA viruses with related replication proteins and could confer resistance to mixed infections and viral variants.

ACKNOWLEDGMENTS

We thank Roger Brent (Molecular Sciences Institute, Berkeley, CA) for providing the pJM-1 peptide library and the corresponding control plasmids and yeast strains used in these studies. We also thank Ling-Jie Kong (Duke University) for technical advice on library amplification and early yeast work and Steffen Hebber and Carla Mattos (NCSU) for advice on alignments and motif identification. We are indebted to Tara Nash and Tamira Butler for their help with the yeast screens and the NCSU Genome Research Laboratory for technical support and advice. We thank the Monsanto Corporation for the gift of pMON10018. We thank Dominique Robertson and Trino Ascencio-Ibanez for critical reading of the manuscript and to members of the Hanley-Bowdoin laboratory for helpful discussions.

This research was supported by grants to L.H.-B. from the Rockefeller Foundation and the North Carolina Biotechnology Center.

REFERENCES

1. **Abramoff, M. D., P. J. Magelhaes, and S. J. Ram.** 2004. Image processing with ImageJ. Biophotonics Int. **11:**36–42.
2. **Ach, R. A., T. Durfee, A. B. Miller, P. Taranto, L. Hanley-Bowdoin, P. C. Zambriski, and W. Gruissem.** 1997. *RRB1* and *RRB2* encode maize retinoblastoma-related proteins that interact with a plant D-type cyclin and geminivirus replication protein. Mol. Cell. Biol. **17:**5077–5086.
3. **Altschul, S. F., T. L. Madden, A. A. Schäffer, J. Zhang, Z. Zhang, W. Miller, and D. J. Lipman.** 1997. Gapped BLAST and PSI-BLAST: a new generation of protein database search programs. Nucleic Acids Res. **25:**3389–3402.
4. **Arguello-Astorga, G., L. Lopez-Ochoa, L.-J. Kong, B. M. Orozco, S. B. Settlage, and L. Hanley-Bowdoin.** 2004. A novel motif in geminivirus replication proteins interacts with the plant retinoblastoma-related protein. J. Virol. **78:**4817–4826.
5. **Arguello-Astorga, G. R., and R. Ruiz-Medrano.** 2001. An iteron-related domain is associated to motif 1 in the replication proteins of geminiviruses: identification of potential interacting amino acid-base pairs by a comparative approach. Arch. Virol. **146:**1465–1485.
6. **Asad, S., W. A. Haris, A. Bashir, Y. Zafar, K. A. Malik, N. N. Malik, and C. P. Lichtenstein.** 2003. Transgenic tobacco expressing geminiviral RNAs are resistant to the serious viral pathogen causing cotton leaf curl disease. Arch. Virol. **148:**2341–2352.
7. **Bogan, A. A., and K. S. Thorn.** 1998. Anatomy of hot spots in protein interfaces. J. Mol. Biol. **280:**1–9.
8. **Boonrod, K., D. Galetzka, P. D. Nagy, U. Conrad, and G. Krczal.** 2004. Single-chain antibodies against a plant viral RNA-dependent RNA polymerase confer virus resistance. Nat. Biotechnol. **22:**856–862.
9. **Brunetti, A., R. Tavazza, E. Noris, A. Lucioli, G. P. Accotto, and M. Tavazza.** 2001. Transgenically expressed T-Rep of tomato yellow leaf curl Sardinia virus acts as a *trans*-dominant-negative mutant, inhibiting viral transcription and replication. J. Virol. **75:**10573–10581.
10. **Butz, K., C. Denk, B. Fitscher, I. Crnkovic-Mertens, A. Ullmann, C. Schroder, and F. Hoppe-Seyler.** 2001. Peptide aptamers targeting the hepatitis B virus core protein: a new class of molecules with antiviral activity. Oncogene **20:**6579–6586.
11. **Butz, K., C. Denk, A. Ullmann, M. Scheffner, and F. Hoppe-Seyler.** 2000. Induction of apoptosis in human papillomavirus-positive cancer cells by peptide aptamers targeting the viral E6 oncoprotein. Proc. Natl. Acad. Sci. USA **97:**6693–6697.
12. **Campos-Olivas, R., J. M. Louis, D. Clerot, B. Gronenborn, and A. M. Gronenborn.** 2002. The structure of a replication initiator unites diverse aspects of nucleic acid metabolism. Proc. Natl. Acad. Sci. USA **99:**10310–10315.
13. **Castillo, A. G., D. Collinet, S. Deret, A. Kashoggi, and E. R. Bejarano.** 2003. Dual interaction of plant PCNA with geminivirus replication accessory protein (REn) and viral replication protein (Rep). Virology **312:**381–394.
14. **Castillo, A. G., L. J. Kong, L. Hanley-Bowdoin, and E. R. Bejarano.** 2004. Interaction between a geminivirus replication protein and the plant sumoylation system. J. Virol. **78:**2758–2769.
15. **Chatterji, A., U. Chatterji, R. N. Beachy, and C. M. Fauquet.** 2000. Sequence

parameters that determine specificity of binding of the replication-associated protein to its cognate site in two strains of Tomato leaf curl virus-New Delhi. Virology **273:**341–350.
16. **Chellappan, P., M. V. Masona, R. Vanitharani, N. J. Taylor, and C. M. Fauquet.** 2004. Broad spectrum resistance to ssDNA viruses associated with transgene-induced gene silencing in cassava. Plant Mol. Biol. **56:**601–611.
17. **Cohen, B. A., P. Colas, and R. Brent.** 1998. An artificial cell-cycle inhibitor isolated from a combinatorial library. Proc. Natl. Acad. Sci. USA **95:**14272–14277.
18. **Colas, P., B. Cohen, T. Jessen, I. Grishina, J. McCoy, and R. Brent.** 1996. Genetic selection of peptide aptamers that recognize and inhibit cyclin-dependent kinase 2. Nature **380:**548–550.
19. **Crawford, M., R. Woodman, and P. K. Ferrigno.** 2003. Peptide aptamers: tools for biology and drug discovery. Brief Funct. Genomic Proteomic **2:**72–79.
20. **Crooks, G. E., G. Hon, J. M. Chandonia, and S. E. Brenner.** 2004. WebLogo: a sequence logo generator. Genome Res. **14:**1188–1190.
21. **Elmer, J. S., L. Brand, G. Sunter, W. E. Gardiner, D. M. Bisaro, and S. G. Rogers.** 1988. Genetic analysis of tomato golden mosaic virus. II. Requirement for the product of the highly conserved AL1 coding sequence for replication. Nucleic Acids Res. **16:**7043–7060.
22. **Estojak, J., R. Brent, and E. A. Golemis.** 1995. Correlation of two-hybrid affinity data with in vitro measurements. Mol. Cell. Biol. **15:**5820–5829.
23. **Fabbrizio, E., L. LeCam, J. Polanowska, M. Kaczorek, N. Lamb, R. Brent, and C. Sardet.** 1999. Inhibition of mammalian cell proliferation by genetically selected peptide aptamers that functionally antagonize E2F activity. Oncogene **18:**4357–4363.
24. **Fauquet, C. M., D. M. Bisaro, R. W. Briddon, J. K. Brown, B. D. Harrison, E. P. Rybicki, D. C. Stenger, and J. Stanley.** 2003. Revision of taxonomic criteria for species demarcation in the family Geminiviridae, and an updated list of begomovirus species. Arch. Virol. **148:**405–421.
25. **Fontes, E. P. B., P. A. Eagle, P. A. Sipe, V. A. Luckow, and L. Hanley-Bowdoin.** 1994. Interaction between a geminivirus replication protein and origin DNA is essential for viral replication. J. Biol. Chem. **269:**8459–8465.
26. **Geyer, C. R., and R. Brent.** 2000. Selection of genetic agents from random peptide aptamer expression libraries. Methods Enzymol. **328:**171–208.
27. **Glaser, F., D. Steinberg, I. Vakser, and N. Ben-Tal.** 2001. Residue frequencies and pairing preferences at protein-protein interfaces. Proteins **43:**89–102.
28. **Golemis, E. A., and R. Brent.** 1992. Fused protein domains inhibit DNA binding by LexA. Mol. Cell. Biol. **12:**3006–3014.
29. **Gutierrez, C.** 1999. Geminivirus DNA replication. Cell. Mol. Life Sci. **56:**313–329.
30. **Gutierrez, C., E. Ramirez-Parra, M. Mar Castellano, A. P. Sanz-Burgos, A. Luque, and R. Missich.** 2004. Geminivirus DNA replication and cell cycle interactions. Vet. Microbiol. **98:**111–119.
31. **Hanley-Bowdoin, L., S. B. Settlage, B. M. Orozco, S. Nagar, and D. Robertson.** 1999. Geminiviruses: models for plant DNA replication, transcription, and cell cycle regulation. Crit. Rev. Plant Sci. **18:**71–106.
32. **Hanley-Bowdoin, L., S. B. Settlage, and D. Robertson.** 2004. Reprogramming plant gene expression: a prerequisite to geminivirus DNA replication. Mol. Plant Pathol. **5:**149–156.
33. **Hanson, S. F., R. A. Hoogstraten, P. Ahlquist, R. L. Gilbertson, D. R. Russell, and D. P. Maxwell.** 1995. Mutational analysis of a putative NTP-binding domain in the replication-associated protein (AC1) of bean golden mosaic geminivirus. Virology **211:**1–9.
34. **Harrison, B., and D. Robinson.** 1999. Natural genomic and antigenic variation in whitefly-transmitted geminiviruses (begomoviruses). Annu. Rev. Phytopathol. **37:**369–398.
35. **Henikoff, S. H., and J. G. Henikoff.** 1992. Amino acid substitution matrices from protein blocks. Proc. Natl. Acad. Sci. USA **89:**10915–10919.
36. **Hoppe-Seyler, F., and K. Butz.** 2000. Peptide aptamers: powerful new tools for molecular medicine. J. Mol. Med. **78:**426–430.
37. **Hoppe-Seyler, F., I. Crnkovic-Mertens, E. Tomai, and K. Butz.** 2004. Peptide aptamers: specific inhibitors of protein function. Curr. Mol. Med. **4:**529–538.
38. **Hou, Y. M., R. Sanders, V. M. Ursin, and R. L. Gilberston.** 2000. Transgenic plants expressing geminivirus movement proteins: abnormal phenotypes and delayed infection by Tomato mottle virus in transgenic tomatoes expressing the Bean dwarf mosaic virus BV1 or BC1 proteins. Mol. Plant-Microbe Interact. **13:**297–308.
39. **Ilyina, T. V., and E. V. Koonin.** 1992. Conserved sequence motifs in the initiator proteins for rolling circle DNA replication encoded by diverse replicons from eubacteria, eucaryotes and archaebacteria. Nucleic Acids Res. **20:**3279–3285.
40. **Kerschen, A., C. A. Napoli, R. A. Jorgensen, and A. E. Muller.** 2004. Effectiveness of RNA interference in transgenic plants. FEBS Lett. **566:**223–228.
41. **Kong, L.-J., and L. Hanley-Bowdoin.** 2002. A geminivirus replication protein interacts with a protein kinase and a motor protein that display different expression patterns during plant development and infection. Plant Cell **14:**1817–1832.
42. **Kong, L.-J., B. M. Orozco, J. L. Roe, S. Nagar, S. Ou, H. S. Feiler, T. Durfee, A. B. Miller, W. Gruissem, D. Robertson, and L. Hanley-Bowdoin.** 2000. A geminivirus replication protein interacts with the retinoblastoma protein through a novel domain to determine symptoms and tissue specificity of infection in plants. EMBO J. **19:**3485–3495.
43. **Koonin, E. V., and T. V. Ilyina.** 1992. Geminivirus replication proteins are related to prokaryotic plasmid rolling circle DNA replication initiator proteins. J. Gen. Virol. **73:**2763–2766.
44. **Lanahan, M. B., H.-C. Yen, J. J. Giovannoni, and H. J. Klee.** 1994. The *never ripe* mutation blocks ethylene perception in tomato. Plant Cell **6:**521–530.
45. **Lapidot, M., and M. Friedmann.** 2002. Breeding for resistance to whitefly-transmitted geminiviruses. Ann. Appl. Biol. **140:**109–127.
46. **Laufs, J., W. Traut, F. Heyraud, V. Matzeit, S. G. Rogers, J. Schell, and B. Gronenborn.** 1995. In vitro cleavage and joining at the viral origin of replication by the replication initiator protein of Tomato yellow leaf curl virus. Proc. Natl. Acad. Sci. USA **92:**3879–3883.
47. **Legg, J. P., and C. M. Fauquet.** 2004. Cassava mosaic geminiviruses in Africa. Plant Mol. Biol. **56:**585–599.
48. **Lucioli, A., E. Noris, A. Brunetti, R. Tavazza, V. Ruzza, A. G. Castillo, E. R. Bejarano, G. P. Accotto, and M. Tavazza.** 2003. *Tomato yellow leaf curl Sardinia virus* Rep-derived resistance to homologous and heterologous geminiviruses occurs by different mechanisms and is overcome if virus-mediated transgene silencing is activated. J. Virol. **77:**6785–6798.
49. **Malik, P. S., V. Kumar, B. Bagewadi, and S. K. Mukherjee.** 2005. Interaction between coat protein and replication initiation protein of Mung bean yellow mosaic India virus might lead to control of viral DNA replication. Virology **337:**273–283.
50. **Mansoor, S., R. W. Briddon, Y. Zafar, and J. Stanley.** 2003. Geminivirus disease complexes: an emerging threat. Trends Plant Sci. **8:**128–134.
51. **McGivern, D. R., K. C. Findlay, N. P. Montague, and M. I. Boulton.** 2005. An intact RBR-binding motif is not required for infectivity of Maize streak virus in cereals, but is required for invasion of mesophyll cells. J. Gen. Virol. **86:**797–801.
52. **Miyake, F., T. Yoshikawa, H. Sun, A. Kakimi, M. Ohashi, S. Akimoto, Y. Nishiyama, and Y. Asano.** 2006. Latent infection of human herpesvirus 7 in CD4(+) T lymphocytes. J. Med. Virol. **78:**112–116.
53. **Moffat, A. S.** 1999. Geminiviruses emerge as serious crop threat. Science **286:**1835.
54. **Morales, F. J.** 2001. Conventional breeding for resistance to Bemisia tabaci-transmitted geminiviruses. Crop Protect. **20:**825–834.
55. **Nagar, S., T. J. Pedersen, K. Carrick, L. Hanley-Bowdoin, and D. Robertson.** 1995. A geminivirus induces expression of a host DNA synthesis protein in terminally differentiated plant cells. Plant Cell **7:**705–719.
56. **Nagel-Wolfrum, K., C. Buerger, I. Wittig, K. Butz, F. Hoppe-Seyler, and B. Groner.** 2004. The interaction of specific peptide aptamers with the DNA binding domain and the dimerization domain of the transcription factor Stat3 inhibits transactivation and induces apoptosis in tumor cells. Mol. Cancer Res. **2:**170–182.
57. **Nauenburg, S., W. Zwerschke, and P. Jansen-Durr.** 2001. Induction of apoptosis in cervical carcinoma cells by peptide aptamers that bind to the HPV-16 E7 oncoprotein. FASEB J. **15:**592–594.
58. **Noris, E., G. P. Accotto, R. Tavazza, A. Brunetti, S. Crespi, and M. Tavazza.** 1996. Resistance to Tomato yellow leaf curl geminivirus in Nicotiana benthamiana plants transformed with a truncated viral C1 gene. Virology **224:**130–138.
59. **Orozco, B. M., and L. Hanley-Bowdoin.** 1996. A DNA structure is required for geminivirus origin function. J. Virol. **270:**148–158.
60. **Orozco, B. M., and L. Hanley-Bowdoin.** 1998. Conserved sequence and structural motifs contribute to the DNA binding and cleavage activities of a geminivirus replication protein. J. Biol. Chem. **273:**24448–24456.
61. **Orozco, B. M., L. J. Kong, L. A. Batts, S. Elledge, and L. Hanley-Bowdoin.** 2000. The multifunctional character of a geminivirus replication protein is reflected by its complex oligomerization properties. J. Biol. Chem. **275:**6114–6122.
62. **Orozco, B. M., A. B. Miller, S. B. Settlage, and L. Hanley-Bowdoin.** 1997. Functional domains of a geminivirus replication protein. J. Biol. Chem. **272:**9840–9846.
63. **Pant, V., D. Gupta, N. R. Choudhury, V. G. Malathi, A. Varma, and S. K. Mukherjee.** 2001. Molecular characterization of the Rep protein of the blackgram isolate of Indian mungbean yellow mosaic virus. J. Gen. Virol. **82:**2559–2567.
64. **Preiss, W., and H. Jeske.** 2003. Multitasking in replication is common among geminiviruses. J. Virol. **77:**2972–2980.
65. **Prins, M., D. Lohuis, A. Schots, and R. Goldbach.** 2005. Phage display-selected single-chain antibodies confer high levels of resistance against Tomato spotted wilt virus. J. Gen. Virol. **86:**2107–2113.
66. **Rasband, W. S.** 2005. Image J. National Institutes of Health, Bethesda, Md.
67. **Real, E., J. C. Rain, V. Battaglia, C. Jallet, P. Perrin, N. Tordo, P. Chrisment, J. D'Alayer, P. Legrain, and Y. Jacob.** 2004. Antiviral drug discovery strategy using combinatorial libraries of structurally constrained peptides. J. Virol. **78:**7410–7417.
68. **Rigden, J. E., I. B. Dry, L. R. Krake, and M. A. Rezaian.** 1996. Plant virus DNA replication processes in *Agrobacterium*: insight into the origins of geminiviruses? Proc. Natl. Acad. Sci. USA **93:**10280–10284.

69. **Rojas, M. R., C. Hagen, W. J. Lucas, and R. L. Gilbertson.** 2005. Exploiting chinks in the plant's armor: evolution and emergence of geminiviruses. Annu. Rev. Phytopathol. **43:**361–394.
70. **Rudolph, C., P. H. Schreier, and J. F. Uhrig.** 2003. Peptide-mediated broad-spectrum plant resistance to tospoviruses. Proc. Natl. Acad. Sci. USA **100:** 4429–4434.
71. **Schmidt, S., S. Diriong, J. Mery, E. Fabbrizio, and A. Debant.** 2002. Identification of the first Rho-GEF inhibitor, TRIPalpha, which targets the RhoA-specific GEF domain of Trio. FEBS Lett. **523:**35–42.
72. **Schneider, T. D., and R. M. Stephens.** 1990. Sequence Logos: a new way to display consensus sequences. Nucleic Acids Res. **18:**6097–6100.
73. **Selth, L. A., J. W. Randles, and M. A. Rezaian.** 2002. *Agrobacterium tumefaciens* supports DNA replication of diverse geminivirus types. FEBS Lett. **516:**179–182.
74. **Sera, T.** 2005. Inhibition of virus DNA replication by artificial zinc finger proteins. J. Virol. **79:**2614–2619.
75. **Settlage, S. B., A. B. Miller, W. Gruissem, and L. Hanley-Bowdoin.** 2001. Dual interaction of a geminivirus replication accessory factor with a viral replication protein and a plant cell cycle regulator. Virology **279:**570–576.
76. **Settlage, S. B., B. Miller, and L. Hanley-Bowdoin.** 1996. Interactions between geminivirus replication proteins. J. Virol. **70:**6790–6795.
77. **Shepherd, D. N., D. P. Martin, D. R. McGivern, M. I. Boulton, J. A. Thomson, and E. P. Rybicki.** 2005. A three-nucleotide mutation altering the Maize streak virus Rep pRBR-interaction motif reduces symptom severity in maize and partially reverts at high frequency without restoring pRBR-Rep binding. J. Gen. Virol. **86:**803–813.
78. **Stajich, J. E., D. Block, K. Boulez, S. E. Brenner, S. A. Chervitz, C. Dagdigian, G. Fuellen, J. G. Gilbert, I. Korf, H. Lapp, H. Lehvaslaiho, C. Matsalla, C. J. Mungall, B. I. Osborne, M. R. Pocock, P. Schattner, M. Senger, L. D. Stein, E. Stupka, M. D. Wilkinson, and E. Birney.** 2002. The Bioperl toolkit: Perl modules for the life sciences. Genome Res. **12:**1611–1618.
79. **Stanley, J.** 2004. Subviral DNAs associated with geminivirus disease complexes. Vet. Microbiol. **98:**121–129.
80. **Sunter, G., M. D. Hartitz, S. G. Hormuzdi, C. L. Brough, and D. M. Bisaro.** 1990. Genetic analysis of Tomato golden mosaic virus: ORF AL2 is required for coat protein accumulation while ORF AL3 is necessary for efficient DNA replication. Virology **179:**69–77.
81. **Tavladoraki, P., E. Benvenuto, S. Trinca, D. de Martinis, A. Cattaneo, and P. Galeffi.** 1993. Transgenic plants expressing a functional single-chain Fv antibody are specifically protected from virus attack. Nature **366:**469–472.
82. **Villani, M. E., P. Roggero, O. Bitti, E. Benvenuto, and R. Franconi.** 2005. Immunomodulation of Cucumber mosaic virus infection by intrabodies selected in vitro from a stable single-framework phage display library. Plant Mol. Biol. **58:**305–316.
83. **Xu, H., P. Zhang, L. Liu, and M. Y. Lee.** 2001. A novel PCNA-binding motif identified by the panning of a random peptide display library. Biochemistry **40:**4512–4520.
84. **Zhang, P., H. Vanderschuren, J. Fütterer, and W. Gruissem.** 2005. Resistance to cassava mosaic disease in transgenic cassava expressing antisense RNAs targeting virus replication genes. Plant Biotechnol. **3:**385–397.